

*Supporting Information*

**Development of a cell permeable ratiometric chemosensor and biomarker for hydrogen sulphate ions in aqueous solution**

Buddhadeb Sen,<sup>a</sup> Manjira Mukherjee,<sup>a</sup> Siddhartha Pal,<sup>a</sup> Sushil Kumar Mandal,<sup>b</sup> Maninder S. Hundal,<sup>c</sup> Anisur Rahman Khuda-Bukhsh<sup>b</sup> and Pabitra Chattopadhyay<sup>a\*</sup>

<sup>a</sup>Department of Chemistry, Burdwan University, Golapbag, Burdwan, 713104, India,

<sup>b</sup>Molecular Biology and Genetics Laboratory, Department of Zoology, Kalyani University, India

<sup>c</sup>Department of Chemistry, Guru Nanak Dev University, Amritsar 143005, India

Corresponding author: [pabitracc@yahoo.com](mailto:pabitracc@yahoo.com)

# CONTENTS

FTIR , $^1\text{H}$ NMR, ESI-MS & $^{13}\text{C}$ NMR spectra of <b>L</b>	<b>Figs. S1a- S1c</b>
FTIR , $^1\text{H}$ NMR, ESI-MS & $^{13}\text{C}$ NMR spectra of <b>L-HSO<sub>4</sub><sup>-</sup></b> species	<b>Figs. S2a - S2c</b>
Naked eye colour change and fluorescence colour change of <b>L</b> in absence and in presence of HSO <sub>4</sub> <sup>-</sup>	<b>Figs. S3 &amp; S6</b>
Absorbance - emission overlay spectra of <b>L</b>	<b>Fig. S4</b>
Effect of pH on <b>L</b> in absence and in presence of HSO <sub>4</sub> <sup>-</sup>	<b>Fig. S5</b>
Different fluorometric plots	<b>Figs. S7 - S10</b>
Partial $^1\text{H}$ NMR spectra for <b>L</b> (10 mM) in presence of varying [HSO <sub>4</sub> <sup>-</sup> ]	<b>Fig. S11</b>
Determination of Binding constant ( <i>K</i> )	<b>Fig. S12</b>
Optimized structure of <b>L</b> and <b>L-HSO<sub>4</sub><sup>-</sup></b> species	<b>Fig. S13</b>
Cytotoxic effect of <b>L</b> in HeLa cells	<b>Fig. S14</b>
Crystal data and details of refinements for C <sub>15</sub> H <sub>12</sub> N <sub>3</sub> O.NO <sub>3</sub>	<b>Table S1</b>
Selected bond distances (Å) and bond angles (°) for C <sub>15</sub> H <sub>12</sub> N <sub>3</sub> O.NO <sub>3</sub>	<b>Table S2</b>
Fluorescence quantum yield ( $\Phi_f$ ) and life time ( $\tau_f$ )	<b>Table S3</b>
HOMO-LUMO energy of <b>L</b> and <b>L-HSO<sub>4</sub><sup>-</sup></b> species	<b>Table S4</b>

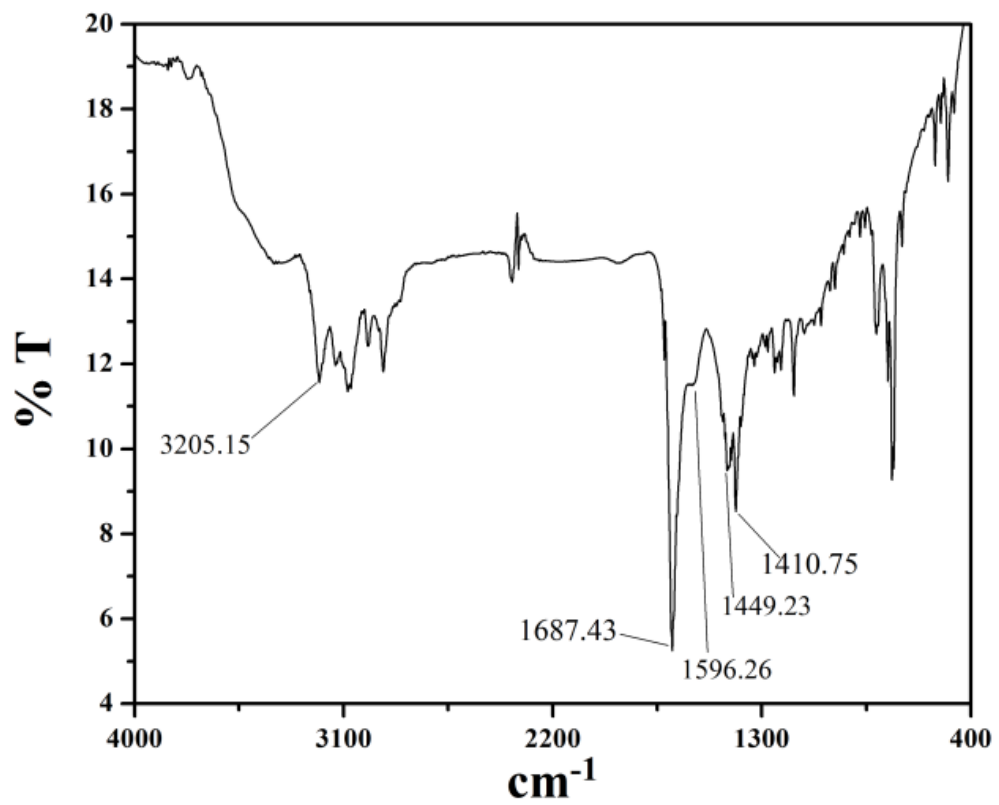


**Fig. S1a** FTIR spectrum of **L**.

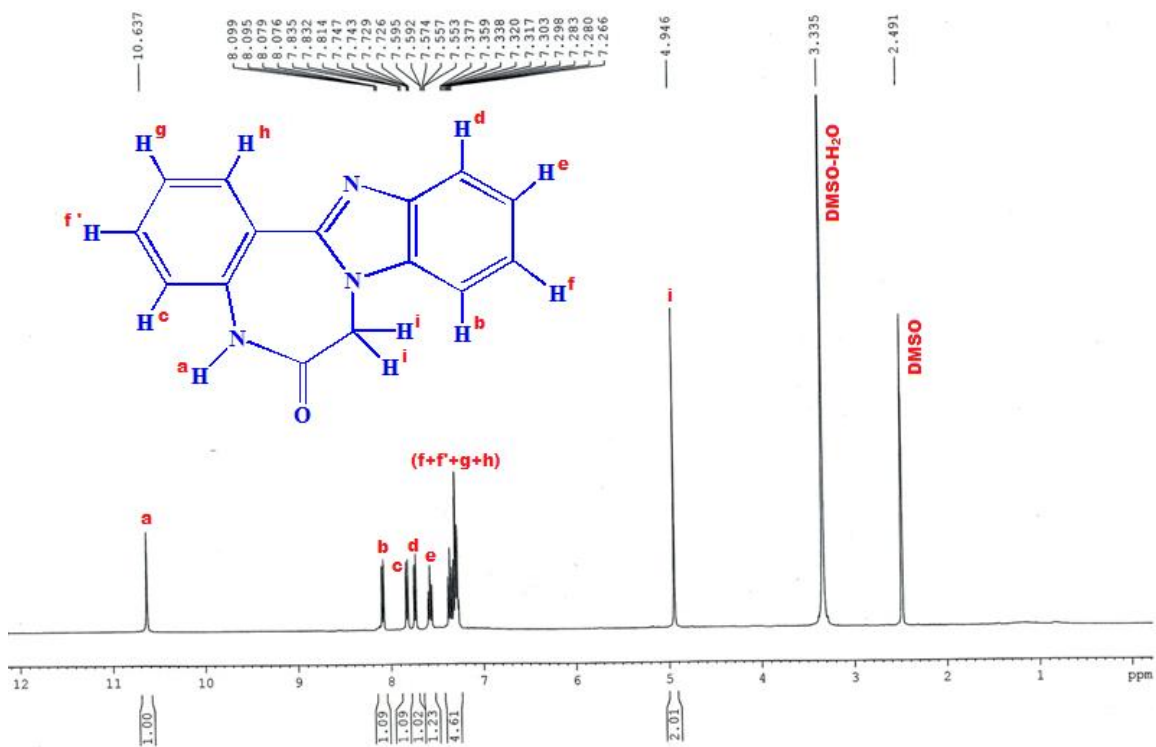


**Fig. S1b**  $^1\text{H}$  NMR spectrum of the probe (**L**) in  $\text{DMSO-d}_6$ .

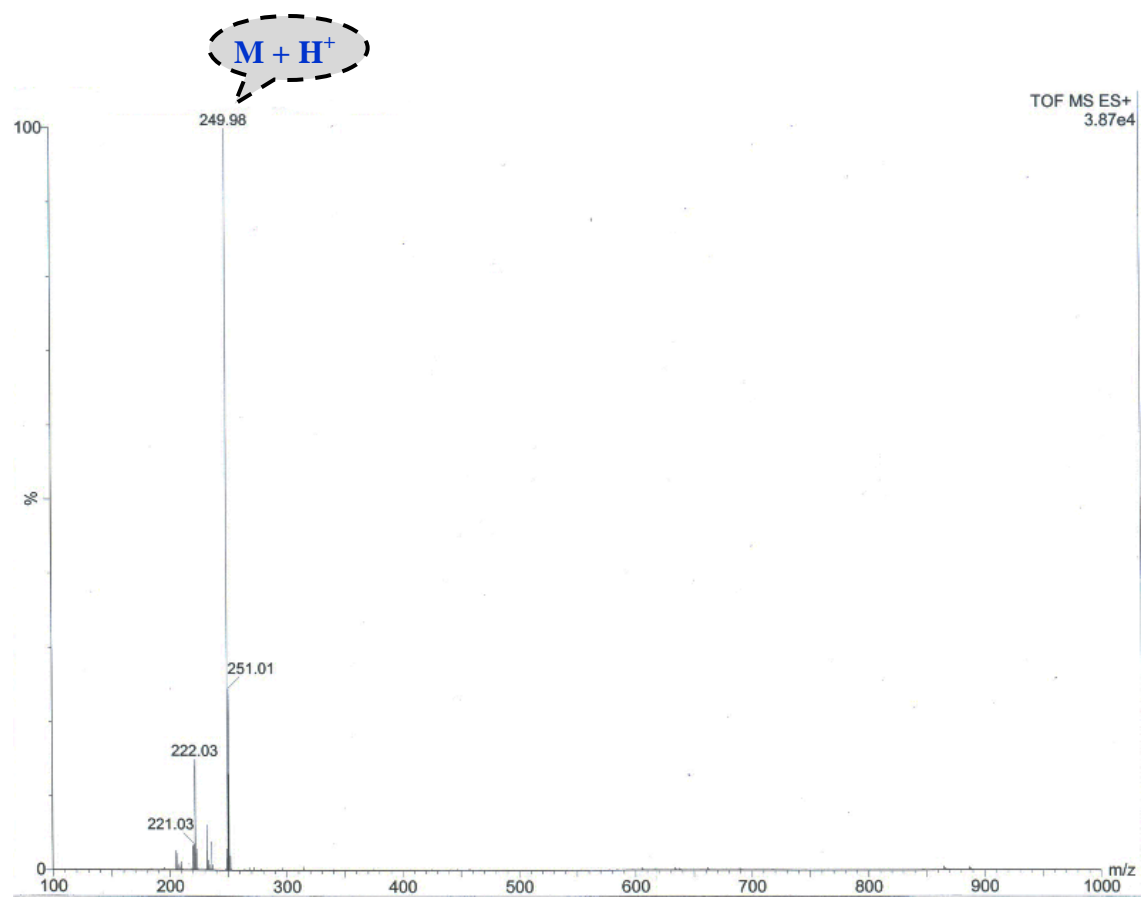


**Fig. S1c** ESI-MS spectrum of probe (**L**).

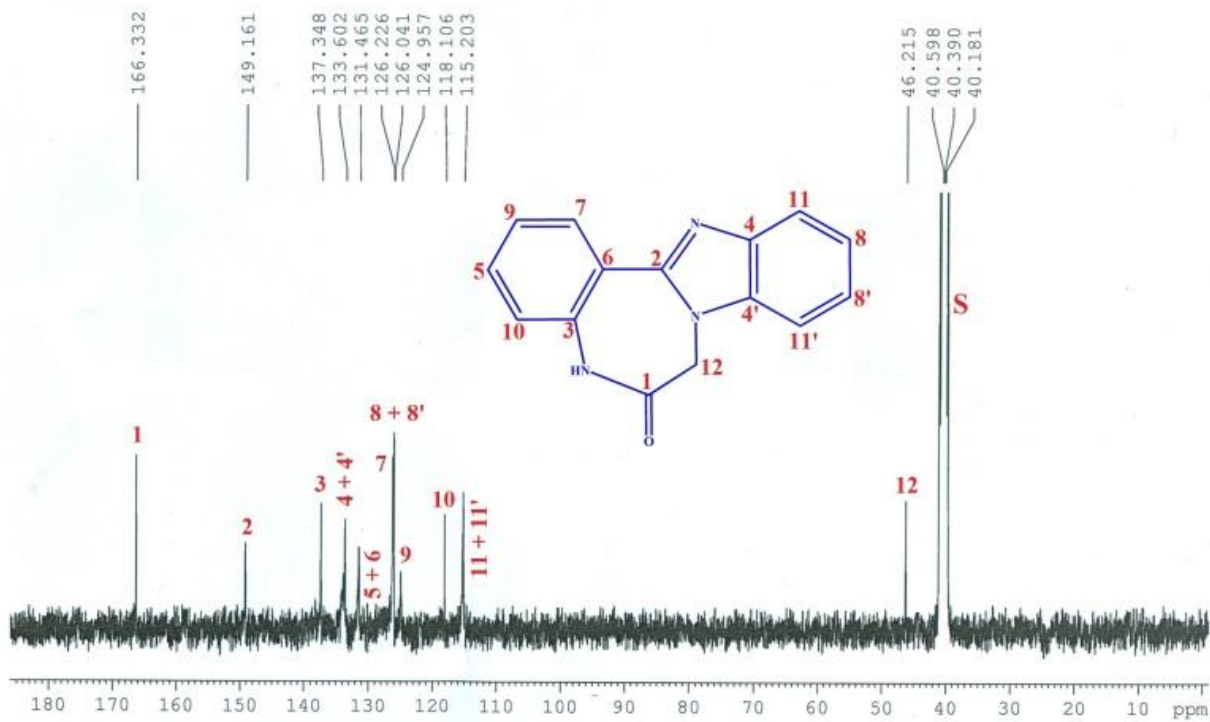


**Fig. S1d**  $^{13}\text{C}$  NMR spectrum of the probe (**L**) in  $\text{DMSO-d}_6$ .

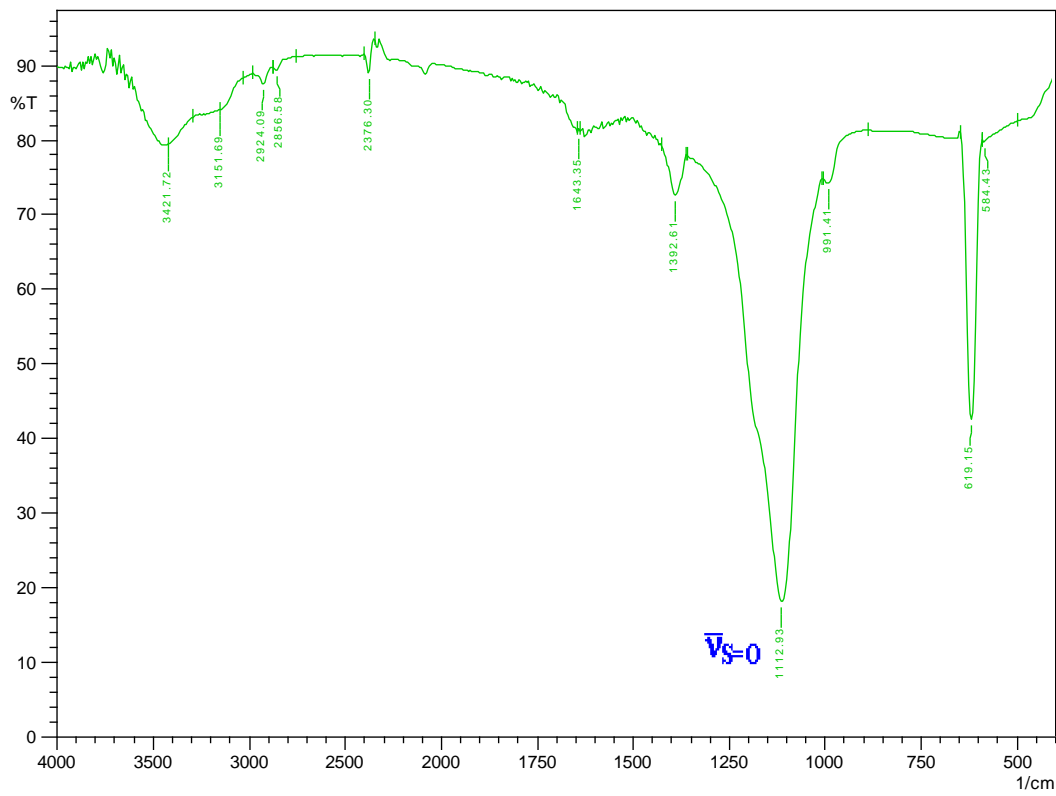


**Fig. S2a** FTIR spectrum of L-HSO<sub>4</sub><sup>-</sup> ensembled species.

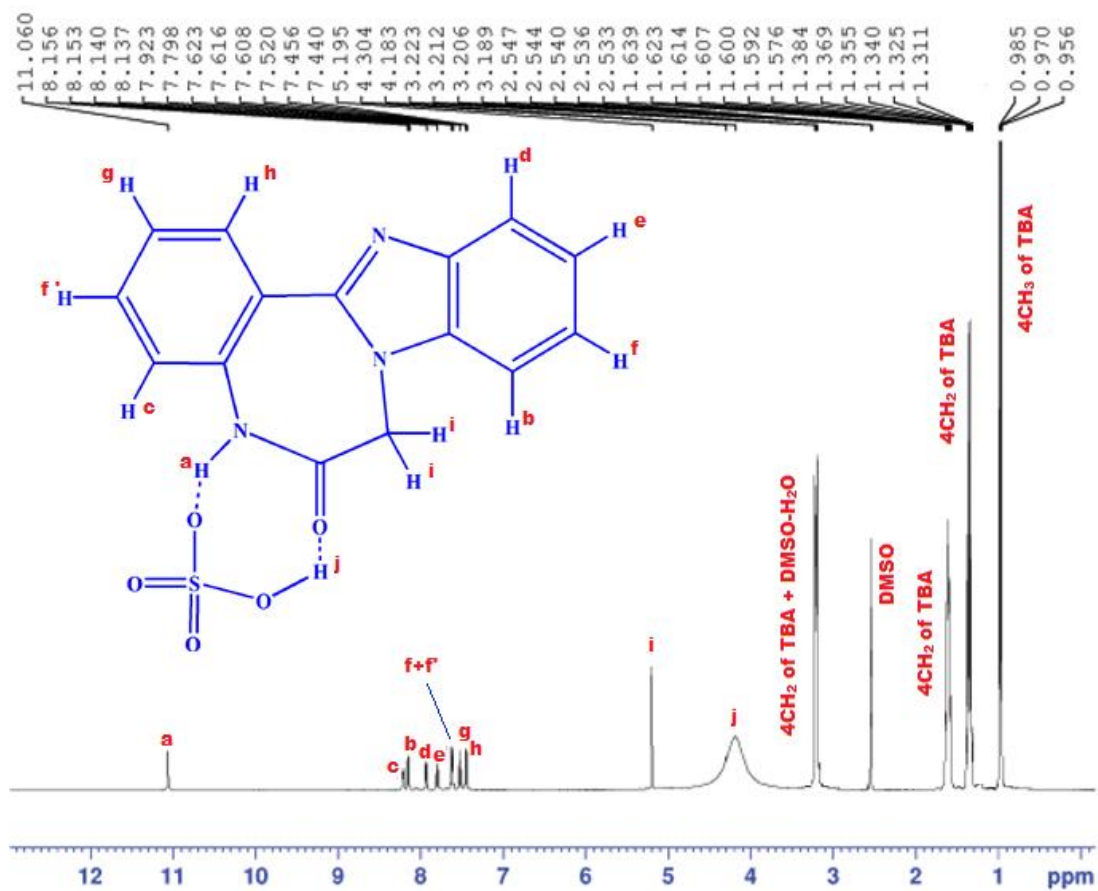


**Fig. S2b**  $^1\text{H}$  NMR spectrum of the species  $\text{L}-\text{HSO}_4^-$  in  $\text{DMSO}-\text{d}_6$ , where TBA= Tetra Butyl Ammonium group.

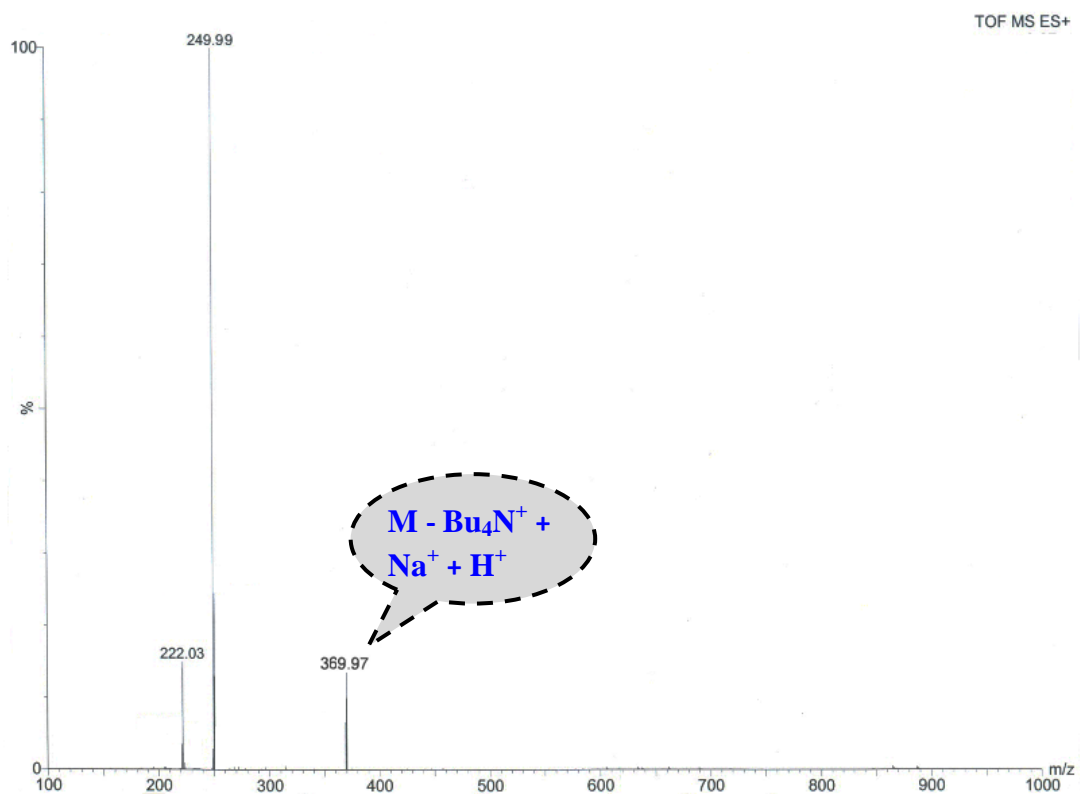


**Fig. S2c** ESI-MS spectrum of  $\text{L}-\text{HSO}_4^-$  species.

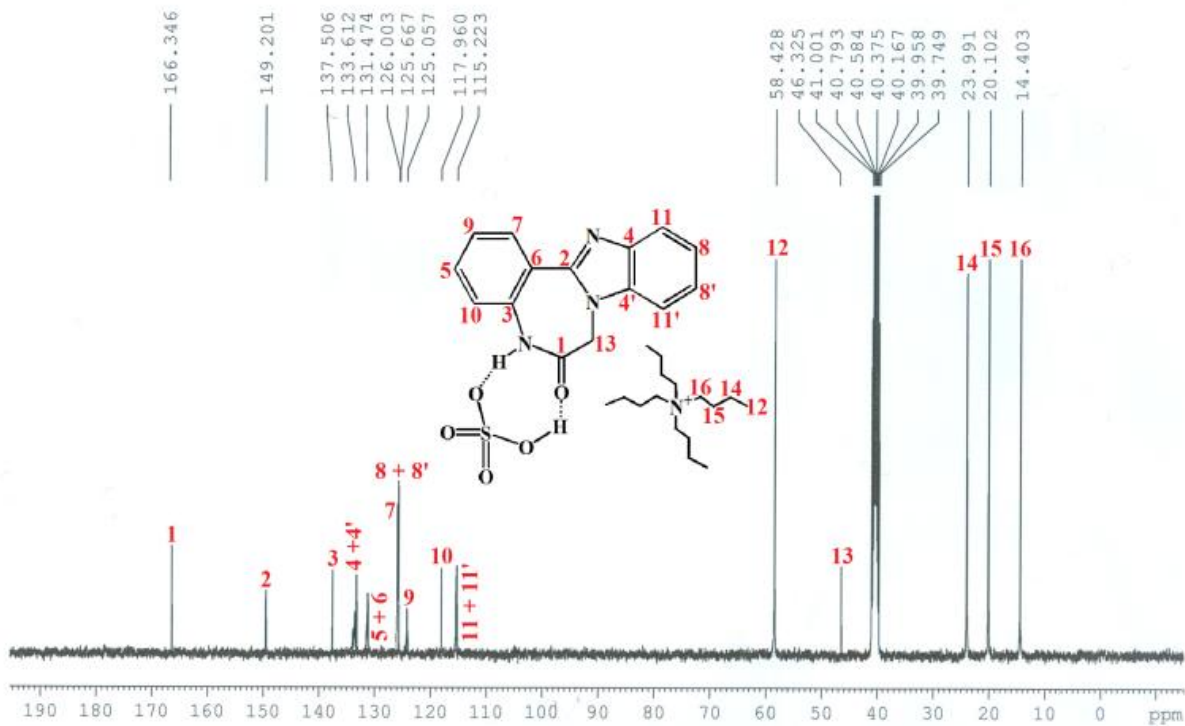


**Fig. S2d**  $^{13}\text{C}$  NMR spectrum of the species  $\text{L}-\text{HSO}_4^-$  in  $\text{DMSO-d}_6$ .

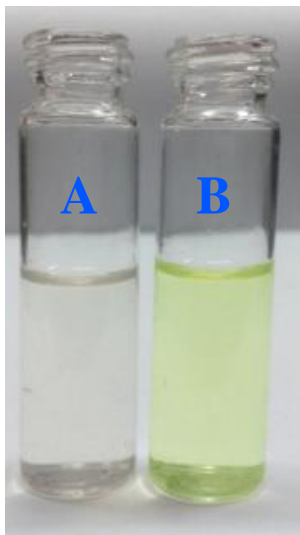


**Fig. S3** Visual colour change of **L**, A) in absence and B) in presence of  $\text{HSO}_4^-$  ions.

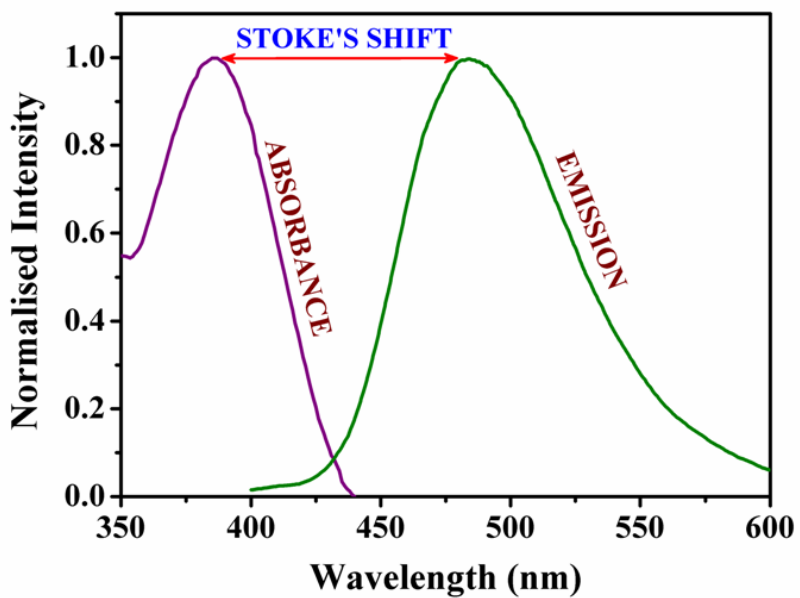


**Fig. S4** Absorbance - emission overlay spectra of **L** ( $10 \mu\text{M}$ ) in HEPES buffer (1 mM, pH 7.4; 2% EtOH) at  $25^\circ\text{C}$ .

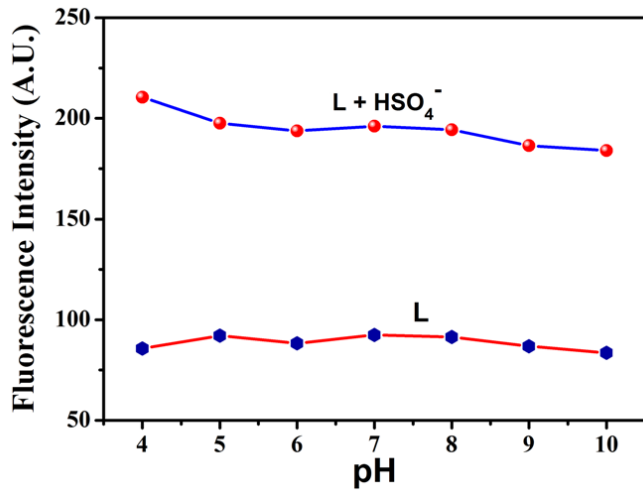


**Fig. S5** Fluorescence response of the **L** in absence / presence of  $\text{HSO}_4^-$  in HEPES buffer (1 mM, 2% EtOH) at 25 °C in different pH at  $\lambda_{\text{em}} = 483\text{nm}$ .

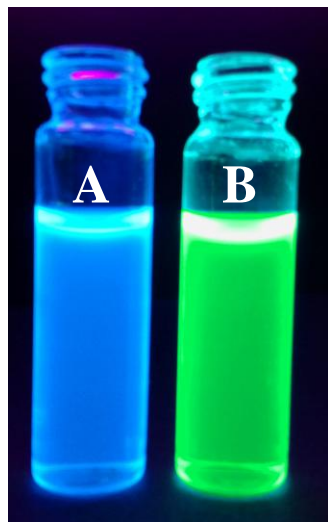


**Fig. S6** Visual fluorescence colour change of **L**, A) in absence and B) in presence of  $\text{HSO}_4^-$  ions in UV light.

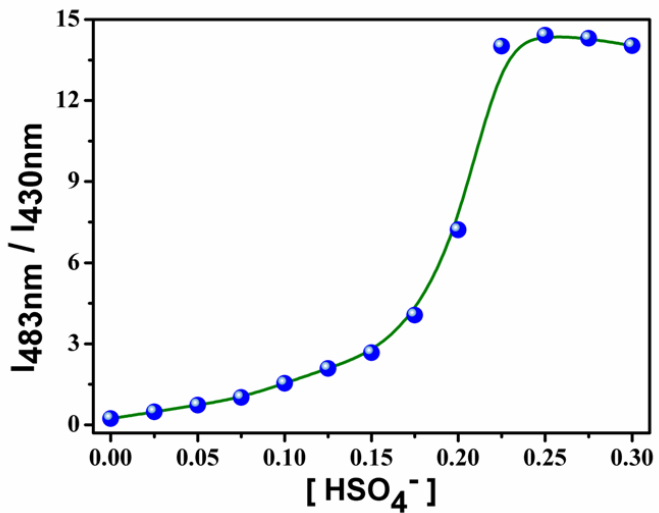


**Fig. S7** Ratiometric signal output of L.

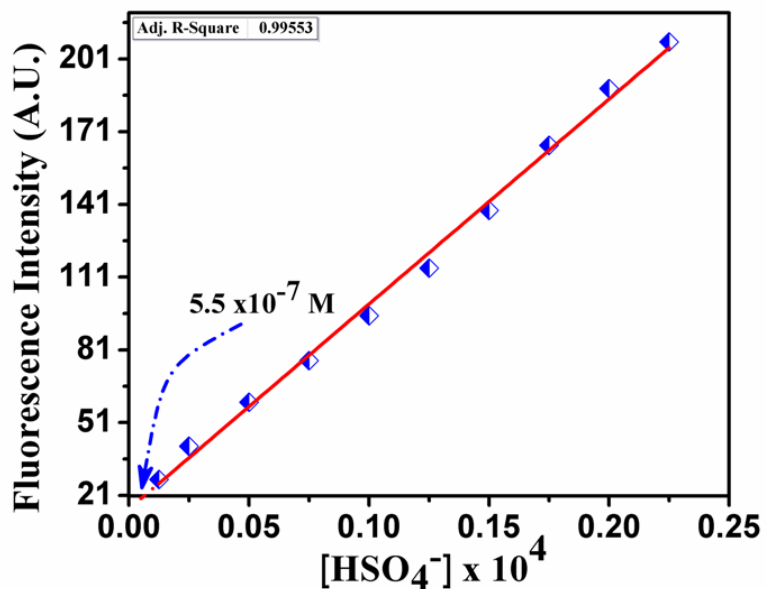


**Fig. S8** Detection limit of HSO<sub>4</sub><sup>-</sup> ions ( $5.5 \times 10^{-7}$  M) in HEPES buffer (1 mM, pH 7.4; 2% EtOH) at 25 °C at  $\lambda_{\text{em}} = 483\text{nm}$ .

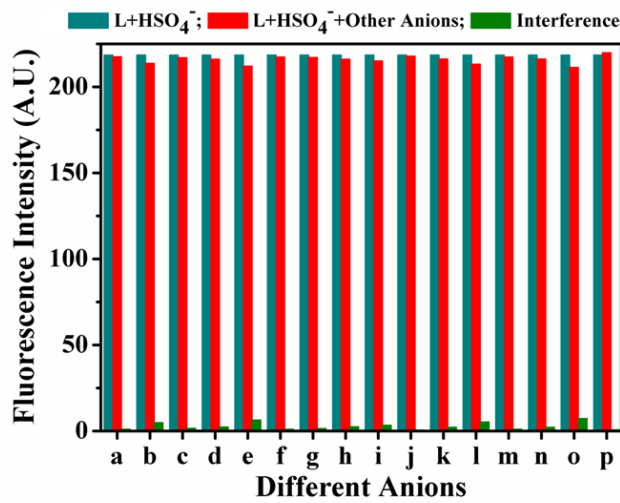


**Fig.S9** Interference of different anions (30  $\mu\text{M}$ ) in presence of **L** (10.0  $\mu\text{M}$ ) and  $\text{HSO}_4^-$  (10.0  $\mu\text{M}$ ) in HEPES buffer (1 mM, pH 7.4; 2% EtOH) at 25 °C where a)  $\text{F}^-$ , b)  $\text{Cl}^-$ , c)  $\text{Br}^-$ , d)  $\text{I}^-$ , e)  $\text{CN}^-$ , f)  $\text{N}_3^-$ , g)  $\text{NO}_3^-$ , h)  $\text{ClO}_4^-$ , i)  $\text{H}_2\text{PO}_4^{2-}$ , j)  $\text{HPO}_4^{2-}$ , k)  $\text{H}_2\text{AsO}_4^-$ , l)  $\text{HAsO}_4^{2-}$ , m)  $\text{AsO}_3^{3-}$ , n)  $\text{OAc}^-$ , o)  $\text{SO}_4^{2-}$ , p)  $\text{S}^{2-}$  at  $\lambda_{\text{em}} = 483\text{nm}$ .

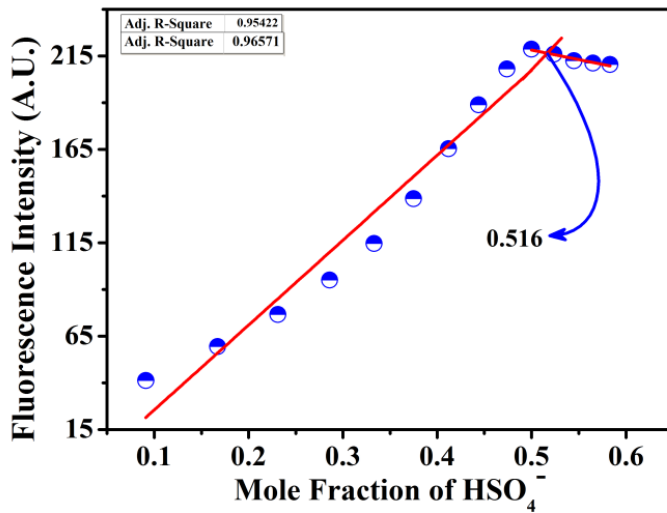


**Fig. S10** Job's plot for stoichiometry determination between **L** and  $\text{HSO}_4^-$  ions from emission intensity showing maximum emission at 1:1 ratio in HEPES buffer (1 mM, pH 7.4; 2% EtOH) at 25 °C at  $\lambda_{\text{em}} = 483\text{nm}$ .

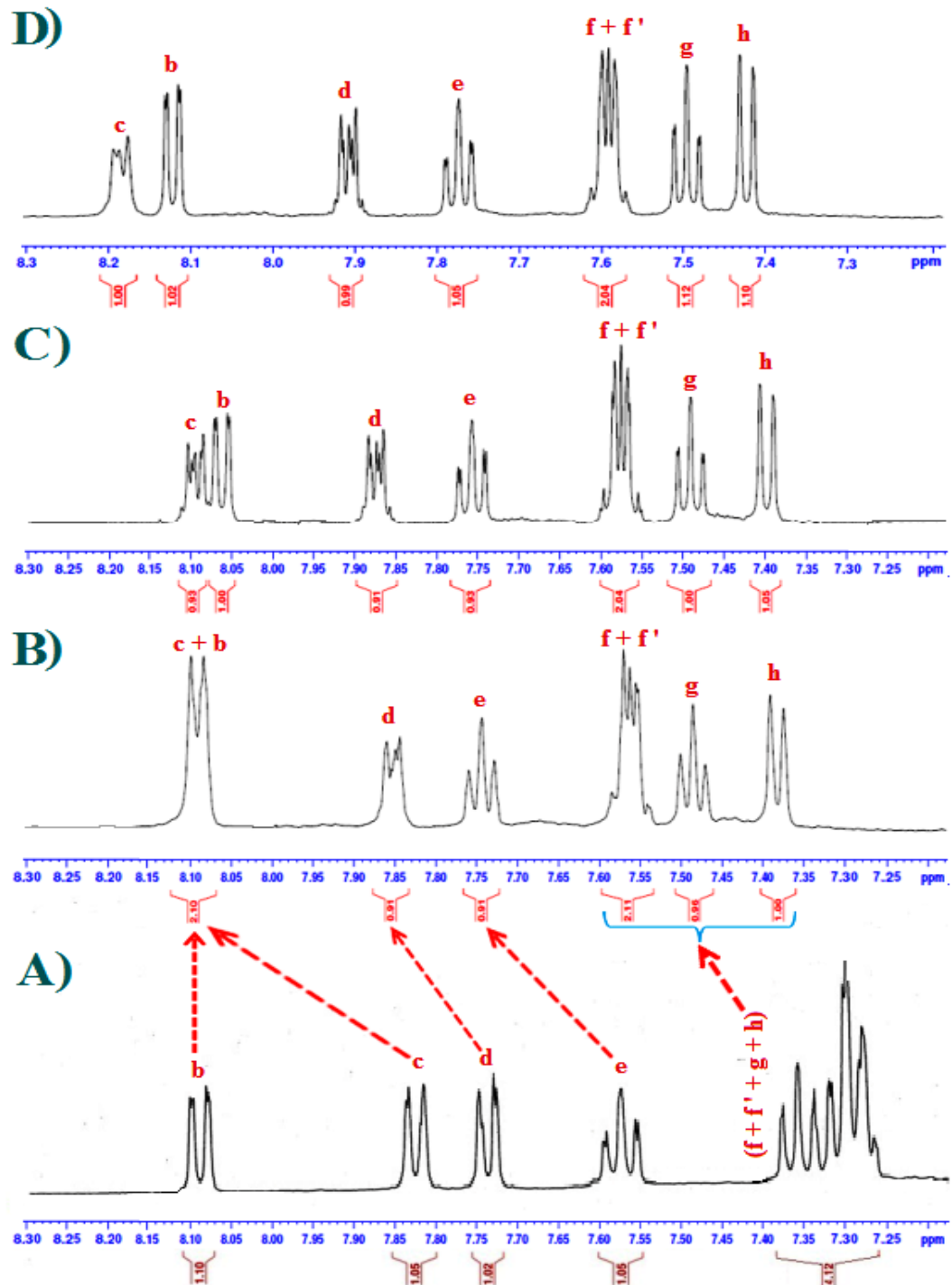


**Fig. S11** Partial  $^1\text{H}$  NMR spectra for **L** (10 mM) in presence of varying  $[\text{HSO}_4^-]$  [ A) 0 mM, B) 3.33 mM, C) 6.67 mM, and D) 10 mM] in  $\text{DMSO-d}_6$ .

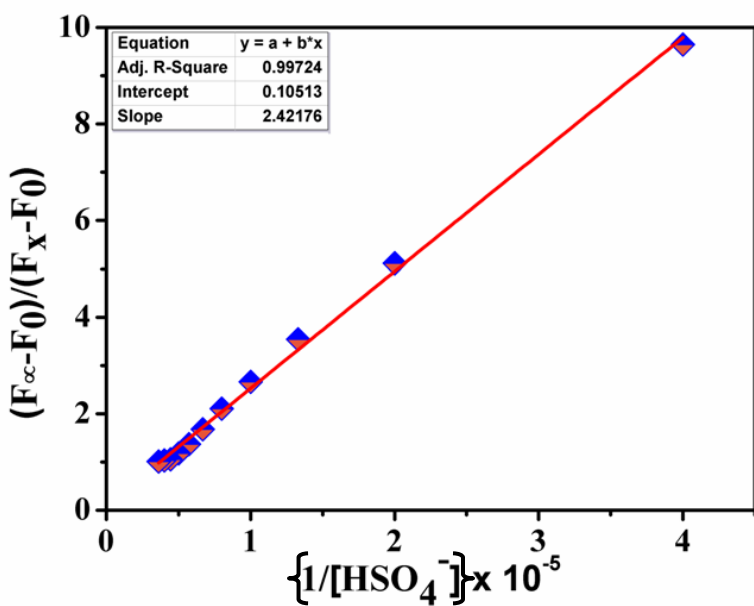


**Fig. S12** Binding constant ( $K$ ) value  $4.13 \times 10^6 \text{ M}^{-1}$  determined from the interaction of **L** with  $\text{HSO}_4^-$  ions in HEPES buffer (1 mM, pH 7.4; 2% EtOH) at 25 °C.



**Fig. S13** Optimized structure of **L** and **L**- $\text{HSO}_4^-$  species.

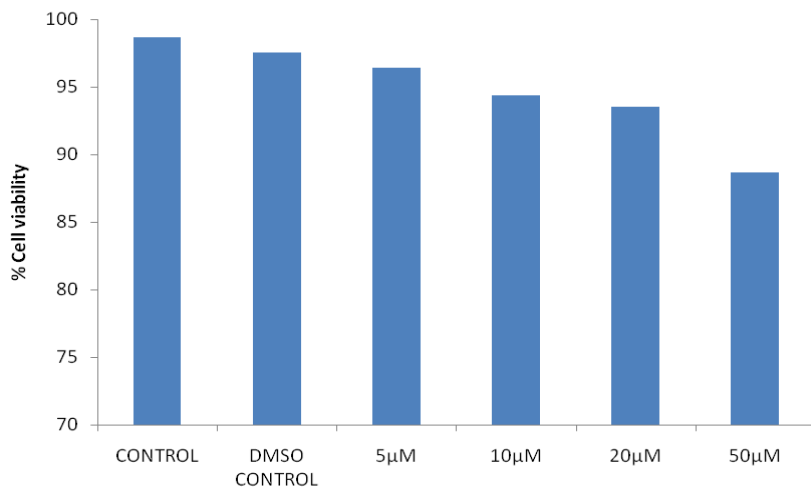


**Fig. S14** Cytotoxic effect of **L** (5, 10, 20, and 50 µM) in HeLa cells incubated for 12 h by MTT assay. Results are expressed as mean of three independent experiments.

**Table S1** Crystal data and details of refinements for C<sub>15</sub>H<sub>12</sub>N<sub>3</sub>O.NO<sub>3</sub>

Empirical Formula	C <sub>15</sub> H <sub>12</sub> N <sub>4</sub> O <sub>4</sub>
Formula Weight	312.09
Crystal System	triclinic
Space group	P-1
a (Å)	7.187(5)
b (Å)	8.453(5)
c (Å)	12.382(5)
α (°)	93.382(5)
β (°)	95.364(5)
γ (°)	107.885(5)
Volume (Å <sup>3</sup> )	709.7(7)
Temperature, K	293(2)
Z	2
ρ <sub>calc</sub> (g/cm <sup>3</sup> )	1.283
F (000)	284
θ range(deg)	1.66 to 28.19°
Collected reflns	12449
Independent reflns	3426
R flns with I > 2σ(I)	2801
R1 [I > 2.0 σ(I)]	0.0421
wR1 [I > 2.0 σ(I)]	0.1262
Goodness-of-fit	0.92

**Table S2** Selected bond distances ( $\text{\AA}$ ) and bond angles ( $^\circ$ ) for  $\text{C}_{15}\text{H}_{12}\text{N}_3\text{O.NO}_3$ 

Bond distances ( $\text{\AA}$ )			
C8-N3	1.3887(18)	C1-N1	1.3557(18)
C9-N3	1.3351(18)	C11-N1	1.4114(17)
C9-N2	1.3455(17)	C1-C2	1.5134(19)
C3-N2	1.3947(17)	C3-C8	1.3920(20)
C2-N2	1.4602(18)	C10-C11	1.4080(20)

Bond angles ( $^\circ$ )			
N1-C1-C2	115.95(12)	N3 C9 C10	126.70(12)
N2-C2-C1	109.73(12)	N2 C9 C10	124.04(12)
C8-C3-N2	106.01(11)	C1 N1 C11	128.78(12)
N3-C8-C3	107.12(11)	C9 N2 C3	108.84(11)
N3-C9-N2	109.26(12)	C3 N2 C2	127.96(11)
O1-C1-N1	122.09(13)	C9 N3 C8	108.74(11)

**Table S3** Fluorescence quantum yield ( $\Phi_f$ ) and life time ( $\tau_f$  in ns) of the corresponding singlet excited states

	$\mathbf{B}_1$	$\mathbf{B}_2$	$\tau_{\text{av}}(\text{ns})$	$\chi^2$	$\varphi$	$\mathbf{k_r}(\mathbf{10^8 s^{-1}})$	$\mathbf{k_{nr} (10^9 s^{-1})}$
<b>L</b>	39.69	60.31	5.77	1.07	0.12	0.2079	0.1525
<b>L+HSO<sub>4</sub><sup>-</sup>(1:0.5)</b>		100	11.79	1.01	0.26	0.2205	0.0628
<b>L+HSO<sub>4</sub><sup>-</sup>(1:1)</b>		100	12.15	1.02	0.45	0.3704	0.0453

**Table S4** HOMO-LUMO energy of **L** and **L-HSO<sub>4</sub><sup>-</sup>** species.

Component	HOMO	LUMO	Difference(a.u.)	Difference(eV)
<b>L</b>	-0.21452	-0.04806	0.16646	4.53
<b>L + HSO<sub>4</sub><sup>-</sup>(Chain)</b>	-0.04630	+0.04798	0.09428	2.57
<b>L + HSO<sub>4</sub><sup>-</sup>(Ring)</b>	-0.09893	+0.03975	0.13868	3.77